Theor Chem Acc (2013) 132:1376
DOI 10.1007/s00214-013-1376-2

REGULAR ARTICLE

Hydrophobic meddling in small water clusters

C. Z. Hadad · Albeiro Restrepo · Samantha Jenkins · Frank Ramírez · Jorge David

Received: 16 April 2013 / Accepted: 3 June 2013 / Published online: 19 June 2013

Abstract What would be the effects on the nature of hydrogen bonds, on the energies, and on the overall structural possibilities of replacing some hydrogen atoms by small hydrophobic groups in small water networks? Aiming at investigating this question, we performed an exhaustive search of the conformational space of the $(Methanol)_2(Water)_3$ representative model system, characterized the results, and made key comparative analysis with pentameric pure water clusters. The potential energy surface yielded a global minimum structural motif consisting of several puckered ring-like cyclic isomers very close in energy to each other. They are followed by other structural motifs, which, contrary to conventional belief, would also contribute to the properties of a macroscopic sample of this composition. We found that the C–H···O interactions play a subordinate structural role and preferably accommodate to the established O–H···O based structures. In comparison with the pure $(H_2O)_5$ case, we showed that (1) the same basic structural motifs and in a similar hierarchy energy order are obtained, but with a richer structural isomerism; (2) in general, the bonding is reinforced by the increase in the electrostatic and in the "degree of covalency" of the hydrogen-bonding components. Therefore, at least for this small cluster size, methyl groups slightly affect the structural isomerism and reinforce the hydrogen bonding. Additionally, we identified general factors of instability of the more unstable structures.

Keywords Methyl group effect · Water–methanol pentameric clusters · Water pentamers · Structure and bonding · Electrostatic and covalent components

1 Introduction

Small hydrogen-bonded molecular clusters have been well studied in the last decades not only because they are interesting from fundamental structural and bonding points of view, but also because they could be models to study the clusters constituents of some interfaces, the gaseous state, and even liquid state and solutions [1–9] and, also, because newly developed experimental techniques have allowed their generation and characterization [1, 3–7, 10–13].

Due to the obvious and broadly recognized and documented importance of water, molecular water clusters are especially attractive to study [13, 14]. Among the smallest water clusters, the cyclic almost planar clusters with homodromic hydrogen-bonding networks, i.e., those exhibiting donor–acceptor arrangements between all water molecules, have special stability due to cooperative effects

Electronic supplementary material The online version of this article (doi:10.1007/s00214-013-1376-2) contains supplementary material, which is available to authorized users.

C. Z. Hadad (✉) · A. Restrepo · F. Ramírez
Instituto de Química, Universidad de Antioquia, A. A., 1226 Medellín, Colombia
e-mail: czhadad@matematicas.udea.edu.co

S. Jenkins
Key Laboratory of Chemical Biology and Traditional Chinese Medicine Research, College of Chemistry and Chemical Engineering, Hunan Normal University, Changsha 410081, Hunan, China

S. Jenkins
Key Laboratory of Resource Fine-Processing and Advanced Materials of Hunan Province of MOE, Hunan Normal University, Changsha 410081, Hunan, China

J. David
Departamento de Ciencias Básicas, Universidad Eafit, A. A., 3300 Medellín, Colombia

[1, 15–18]. This is the case for the water trimer, W_3, water tetramer, W_4, and water pentamer, W_5, clusters, where cyclic clusters are the global minima. Hexamer water clusters, W_6, constitute the transition between planar and three-dimensional configurations, where prism- and cage-like configurations are the global minima [19]. Experimental and theoretical data indicate that the hydrogen-binding energies (BE) per hydrogen bond increase relatively little (due to the cooperative effects) when going from the global minimum W_3 to the global minimum W_4, or from the global minimum W_4 to the global minimum W_5, but it decreases abruptly from W_5 to W_6 global minimum, even though the ratio (number of hydrogen bonds)/(number of water molecules) increase when going from W_3 or W_4 or W_5 to W_6 [1, 15–18, 20]. The cooperative effect is an additional stabilizing factor where the individual bonds are reinforced by a better redistribution of the total electron density and of the collection of bond dipoles involved in clusters bonding, and where non-additive three body terms are at play [15, 21, 22].

Owing to the possibility of forming cyclic structures with cooperative stabilizing effects, small hydrogen-bonded molecular clusters (water-like molecules, R–OH) of sizes smaller than 6 are particularly attractive to study. For example, we can examine the effect of replacing one or more H atoms for hydrophobic groups. Questions that arise are as follows: What is the effect of allowing the possibility to form weaker interactions of the C–H···O type by replacing hydrogen atoms in water by, for example, methyl groups? Will they form different structures relative to the water clusters? What would be the net effect of the methyl groups on each bond and on the overall clusters? Aiming at investigating those questions, we have chosen in this study the pentameric water system (with the possibility of forming cyclic cluster with the largest hydrogen-binding energy per hydrogen bond) and replaced 2 water molecules by methanol. We performed an exhaustive search of the potential energy surface, PES, in order to find as many isomers as possible. We then characterized the structure and bonding of the resulting clusters relative to pure water pentamers. In this article, we will use the M_2W_3 and W_5 nomenclature to refer to the methanol–water and water pentamers, respectively. The M_2W_3 system was chosen because is the pentameric cluster with the minimum number of replacements that permits including the possibility of interaction between methyl groups (for completeness).

A very interesting report about water–methanol cluster was published by Subramanian et al. [23], who made a theoretical study about methanol, water, and methanol–water mixed clusters (M_mW_n, where $m = 0$–4 and $n = 0$–4; $m + n = 4$) at the HF, DFT (B3LYP), and MP2 levels of theory. The authors reported some of the more probable structures, including the more stable ones, which correspond to cyclic structures in the case of trimers and tetramers. Their results and analysis using Bader's quantum theory of atoms in molecules, natural bond orbital analysis, and reduced variational space decomposition analysis show that BEs of methanol and mixed clusters, and the cooperative stabilization are higher than those of pure water clusters due to the electron-donating nature of the methyl group. Even though the paper of Subramanian et al. [23] lacks of an exhaustive non-guessing dependent search of the PES (as we intend to do in this study for the pentameric cluster), their findings are relevant to our study.

Other important experimental and theoretical previous studies on methanol–water clusters concluded that in these systems, CH_3OH acts preferably as proton acceptor and H_2O as proton donor in the more stables isomers [24–27]. For example, using microwave rotation-tunneling spectroscopy of water–methanol dimer formed in supersonically cooled molecular beams, Stockman et al. [24] demonstrates unambiguously that the lower-energy conformation corresponds to a water-donor, methanol-acceptor complex, conclusion that was also reached theoretically by Iousue et al. [25], using rigid-body diffusion Monte Carlo methods, and by Jursic [26] using several ab initio methods.

On the other hand, studies on ethanol–water systems [27–30] indicate that the ethyl group of ethanol contributes to the cooperative stabilization of the clusters, and the most stable clusters for small systems are also cyclic ones.

Finally, it is necessary to add that the methanol–water system is interesting because it could have implications in the development of efficient fuel cells [31], and it is used as anti-detonant injection mixture for internal combustion engines [32] and as mobile phases in high-performance liquid chromatography [33], among others.

2 Computational methods

To generate candidate structures, we used the after its acronym Annealing Simulado Con Energía Cuántica (ASCEC) program in its molecular cluster capabilities [21, 34]. ASCEC contains a modified Metropolis acceptance test in an adapted version of the simulated annealing optimization procedure. We used the big bang approach to construct the initial geometries for all ASCEC runs: the five molecules, two methanol, and three waters were placed at the same position allowing them to evolve under the annealing conditions. The systems were placed inside cubes of 8 Å of length. The PM3 semiempirical Hamiltonian was used to calculate the energy of a Markovian chain of randomly generated pentamer configurations. We used geometrical quenching routes with initial temperature of 500 K, a

constant temperature decrease of 5 %, and 100 total temperatures. We did 4 independent ASCEC runs to ensure a good scan of the potential energy surface, PES. The hybrid B3LYP density functional in conjunction with the 6–31 + G(d) basis set was used to optimize and characterize, in a first step, the structures afforded by ASCEC. Further optimization, refinement, and characterization of the stationary points were carried out by using second-order perturbation theory at the MP2/6–311 ++G(d, p) level. Analytical harmonic second-order derivative calculations were used to characterize all stationary points as true minima (no negative eigenvalues of the Hessian matrix) at the same theory level. Highly correlated CCSD(T) energies were calculated on all the MP2 located minima using the 6–311 ++G(d, p) basis set.

This methodology has been successfully used in the study of small hydrogen-bonded networks, specifically the water tetramer [21], pentamer [22], hexamer [19], the methanol tetramer [35], and the carbonic acid dimer [36]. A detailed description of the workings of the ASCEC algorithm is found in Ref. [21].

Binding energies were calculated by subtracting the energy of the given pentamer cluster from its component isolated monomers, in this way, larger positive numbers correspond to larger stabilization energies. We used the MP2/6–311 ++G(d, p) ZPEs to correct the CCSD(T) electronic energies in the calculations of BE and relative stabilities. There are several reports that clearly reveal the failure of counterpoise correction for basis set superposition error in the study of small hydrogen-bonded clusters; specific cases are the dimers of carbonic acid $(H_2CO_3)_2$ [36, 37], hydrofluoric acid HF_2 [38, 39], and water $(H_2O)_2$ [40]. Theoretical treatment of the methanol tetramer [35] showed no significant differences by correcting for BSSE. Therefore, in this work, we restrain ourselves from applying such methodology. All optimization, frequency, and energy calculations were carried out using the Gaussian 03 suite of programs [41]. Reference Boltzmann populations were estimated by standard Boltzmann distribution analysis [21]. All the QTAIM properties were calculated using AIMQB program within the AIMStudio [42] suite, using the Proaim basin integration method.

3 Results and discussion

3.1 Structures, energies, and stabilization

After the ASCEC–optimization–refining process, we found 164 distinct molecular clusters corresponding to local minima on the MP2/6-311 ++G(d, p) PES (see Online resource for their Cartesian coordinates). Our results indicate that the hydrogen bonds of the O–H···O type, which we called "primary hydrogen bonds," PHBs (hydrogen bonds in the classical sense), are responsible for the basic structural skeleton, and the C–H···O interactions, which we called "secondary hydrogen bonds," SHBs, play a subordinated structural role. A classification of the clusters by PHB structures leads to 11 basic structural motifs which, to facilitate the comparison, we name similarly to the W_5 case of our previous study in Ref. [22]: puckered ring, envelope, tetramer/trimer, tricycle, tetramer + 1, chain, double trimer, trimer + 2, bicycle + 1, and trimer + 1 + 1 cis and trans (see Fig. 1; Table 1). Each structural motif is enriched by the several conformational possibilities for molecular fragments that form the network holding the same motif. Additionally, many structures show some possibilities for SHBs between the hydrogen atoms bonded to the carbon atoms and the oxygen atoms of other molecules. In Fig. 1, some selected structures, including a representative cluster for each motif, are shown in decreasing order of stability according to the CCSD(T)//MP2 energies. The PHBs are indicated as fat dot lines, while the SHBs by thin ones. In this figure, we indicated only the most obvious SHBs. A more rigorous designation of binding is possible with Bader's QTAIM [43], as we will see later.

To illustrate some structural facts that give rise to the diversity of possibilities, for the puckered ring motif, we show 5 different isomers in Fig. 1. The only difference between the puckered ring isomers 1 and 2 is the alternation to one or the other side of the ring plane of one of the peripheral free hydrogens (not taking part in the HB network). In the same manner, puckered ring isomer 3 shows the possibility of having clusters with equally oriented methyl groups, in contrast to the plane-opposed methyl groups of isomers 1 and 2. In puckered ring isomers 4 and 5, methyl groups are further apart from one another, allowing the possibility of optical isomerism.

Note that the alternation of the peripheral hydrogens or of the methyl groups to one side or the other of the puckered ring plane reveals that the lone electron pair (within the Lewis–VSEPR simplified view [44] and the peripheral group (-H in water and methanol, or $-CH_3$ in methanol) that fall outside of the PHB structural skeleton may be interchanged, giving rise to many structural possibilities.

Table 1 shows energetic and stabilization data for some selected clusters, listed by motif groups and in decreasing stability order. The structural motifs from puckered ring to tetramer + 1(b) correspond to the totality of the most stable clusters found (structures that sum approximately the 99.9 % of the Boltzmann reference population). The group from chain to trimer + 1 + 1 trans is a selection, as example, consistent of one structure for each of the remaining motifs.

The puckered ring motif is the global minimum and consists of several structures very close in energy between

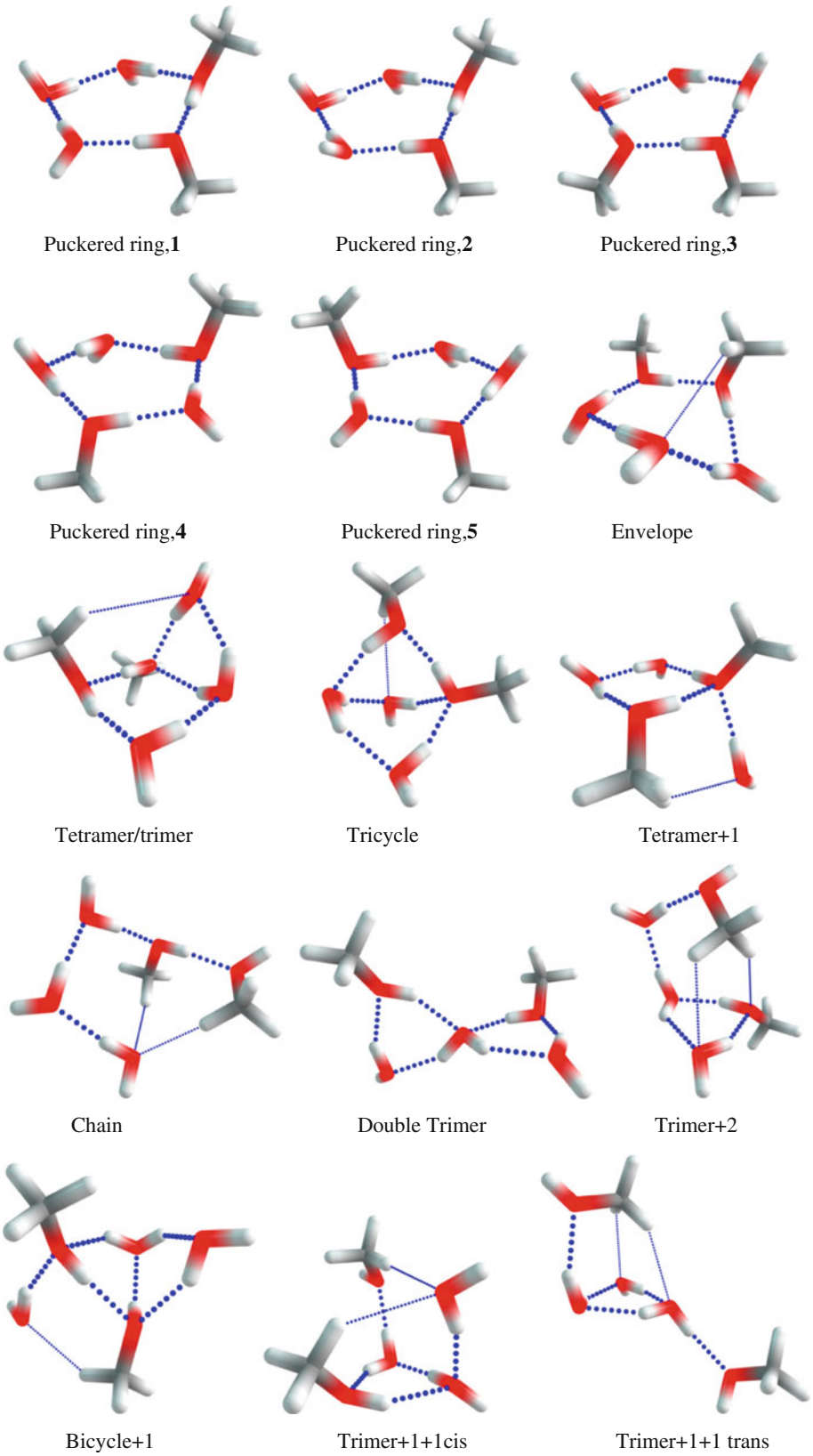

Fig. 1 A sample of the PES energy minima structures obtained in our search optimization process. The PHBs are indicated as fat *dotted lines*, while the SHBs by *thin ones*

them. They add up to 88 and 92 % of the Boltzmann reference population at CCSD(T) and MP2 levels, respectively. We found 11 puckered ring structures within an energy range of 0.28 kcal/mol, i.e., within a range where it is difficult to secure a statement about differences and hierarchies in stability, due to computational uncertainty [45].

Table 1 Energetic data for the M_2W_3 clusters

Motif	N° of structures found	SHB?	ΔE (range or value) CCSD(T)	ΔE (range or value) MP2	BE (range or value) CCSD(T)	BE (range or value) MP2	Ref. Pop. % CCSD(T)	Ref. Pop. % MP2
Puckered ring	11	No	0.00–0.28	0.00–0.29	32.53–32.81	33.34–33.63	88.3	92.2
Envelope	2	Yes	0.98–1.10	1.10–1.19	31.71–31.83	32.44–32.53	3.2	2.8
Tetramer/trimer (a)	4	Yes	1.21–1.45	1.51–1.74	31.37–31.60	31.89–32.13	4.0	2.5
Tricycle (a)	2	Yes	1.51–1.67	1.89–2.10	31.15–31.30	31.53–31.74	1.3	0.7
Tetramer/trimer (b)	2	No	1.70–1.73	2.02–2.12	31.08–31.11	31.51–31.61	1.0	0.6
Tricycle (b)	2	Yes	1.87–1.95	2.27–2.39	30.86–30.94	31.24–31.36	0.7	0.4
Tetramer/trimer (c)	1	No	2.15	2.45	30.66	31.18	0.3	0.2
Tricycle (c)	2	Yes	2.28–2.30	2.74–2.75	30.51–30.53	30.88–30.90	0.4	0.2
Tetramer + 1 (a)	1	Yes	2.35	2.6	30.46	31.03	0.2	0.1
Tricycle (d)	2	Yes	2.42–2.48	2.87–2.91	30.33–30.39	30.72–30.76	0.3	0.2
Tetramer/trimer (d)	1	Yes	2.55	2.95	30.27	30.68	0.1	0.1
Tetramer + 1 (b)	1	Yes	2.83	3.06	29.98	30.57	0.1	~0.0
Chain	–	Yes	6.01	6.29	26.81	27.34	~0.0	~0.0
Double trimer	–	No	6.05	6.52	26.76	27.11	~0.0	~0.0
Trimer + 2	–	Yes	6.68	7.18	26.13	26.45	~0.0	~0.0
Bicycle + 1	–	Yes	7.08	7.86	25.73	25.78	~0.0	~0.0
Trimer + 1 + 1 cis	–	Yes	7.43	7.96	25.39	25.67	~0.0	~0.0
Trimer + 1 + 1 trans	–	Yes	10.29	10.88	22.52	22.75	~0.0	~0.0

SHB: Secondary hydrogen bonds (C–H···O). ΔE: Relative energies with respect to the most stable structure at each level of theory. BE: Binding energy. All CCSD(T)/6-311 ++G(d,p) calculations using the MP2/6-311 ++G(d,p) optimized geometries. All relative and binding energies are in kcal/mol and are corrected for the unscaled MP2/6-311 ++G(d,p) ZPEs. The reference isomer contributions, Ref. Pop. %, estimated via Boltzmann population analysis

Therefore, the interchange of the alternation order, of the peripheral -H or -CH_3 groups, to one or the other side of the plane, maintaining the puckered ring motif, incorporates, in rough terms, no difference in stability. Likewise, to be (1, 2) or (1, 3) with respect to the mutual disposition of methyl groups does not provide significant differences in stability. It seems that what really provides the stability to this kind of structure is the favorable sequence of bond dipoles, δ(−)O–Hδ(+), that make up the cooperative system of hydrogen bonds. In previous works [19, 21, 22], we observe that the disposition of bond dipoles is pivotal in determining stability and diversity of motifs in water clusters. The M_2W_3 case obeys the same tendency: For 5 bond dipoles, the sequence of five dipole–dipole interactions in an almost planar ring, when each molecule is only once H donor and once H acceptor leading to the most stable spatial arrangement, as we can see in Fig. 1, where the structures as sticks colored differently at the end of the bonds, facilitates the view of the constituent bond dipoles. However, the fact of having a diversity of up and down peripheral –H and –CH_3 groups with respect to the ring plane and that this molecular plane is puckered in the most stable structure indicate us that we must take into consideration that the negative, δ(−)O−, side of the bond dipole has two positions to accept the positive, −Hδ(+), side of another molecule: according to the simplified Lewis–VSEPR view [44], those positions correspond to the 2 lone electron pairs, which are approximately 109.5° apart. The 2 lone electron pairs are available to "align" with the −Hδ(+) side to build many isomers as the number of possible combinations. This simplified view could help us to explain structural aspects such as the directionality of the HBs in these R-OH systems and the diversity of structures found.

We can observe that all puckered ring structures have the hydrogen atoms and the methyl groups not taking part in the stabilizing hydrogen-bonding network alternated relative to their position to one side or the other side of the cluster plane, but, as there are 5 groups, 2 adjacent groups must be at the same side. When there are three contiguous groups on the same plane side of this five members ring, the structure loses its planarity considerably and thus the stability of the dipole sequence and becomes the envelope motif (see Fig. 1) that is approximately 1 kcal/mol more energetic. Envelope structures constitute about 3 % of the reference Boltzmann population. When the cause of this loss of planarity is an additional PHB between two molecules inside the ring, the puckered ring cluster transforms into the tetramer/trimer motif, which is 1.2–3.0 kcal/mol more energetic, depending on the case.

In the tetramer/trimer case, we observe that in addition to the loss of planarity, an additional instability factor arises when one or more molecules of the cluster become a double H donor (in the water case) or double H acceptor (water and methanol cases), which appears to weaken the PHBs systems. This is the case for the motifs that follow in stability, except for the chain-like structures, which must be discussed separately.

We can observe in the last structures of Fig. 1, and in the last part of Table 1 that the least stable non-chain-like structures consist of small rings of four and three members. This is an additional instability factor due to the stress introduced in comparison with the puckered ring structure. Likewise, the planarity loss and shrinking of rings are instability factors probably due to the loss of a more favorable dipole distribution. The double H donor and/or double H acceptor character of one molecule of the cluster reduces the strength of the each HB, by "electron density dilution," resulting in an overall stability reduction in the system.

Talking about good or bad dipole distributions suggests doing an energy decomposition analysis to verify the direct relationship between the stability and the electrostatic energy component. The Su and Li scheme [46] provides a suitable method where the Hartree–Fock interaction energy (within a supermolecule calculation) is decomposed into electrostatic (ES), exchange (EX), repulsion (REP), and polarization terms (PL), and where it is possible to add a dispersion term (DISP) within, for example, the second-order Møller–Plesset perturbation method. For the clusters of Table 1, we found that the ES component ranges between −80 and −51 kcal/mol, the EX component between −94 and −55 kcal/mol, the REP component between +170 and +98 kcal/mol, the PL component between −31 and −15 kcal/mol, and the MP2 DISP component between −12 and −9 kcal/mol. The larger numbers (in absolute value) of those ranges are for the more stable structures (starting from puckered ring), and the smaller ones are for the least stable structure (ended at the trimer + 1 + 1 trans motif). A plot showing the correlation between the ZPE corrected CCSD(T) BEs and ES Su and Li component is shown in Fig. 2. We can observe that the cluster stability (BE values) largely increases with the ES energy content, which evidence the importance of the electrostatic factor in the stability of this kind of systems. In the same plot, we have included the PL component, which increases (in absolute value) with BE, but more smoothly than the ES component. In this decomposition scheme, PL component is equivalent to the sum of the polarization, charge transfer, and mixing term in the Kitaura–Morokuma energy decomposition analysis [47]. Therefore, the stability of the clusters also increases as the degree of the HB covalency increases, mainly due to the charge transfer component, as indicated

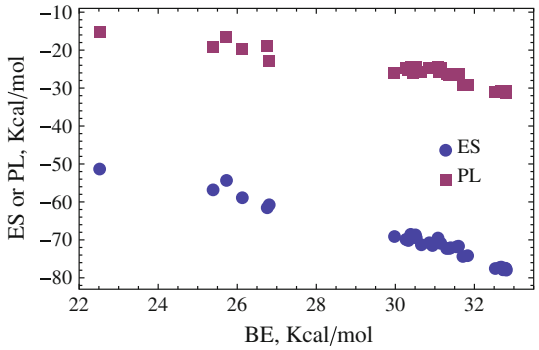

Fig. 2 Correlation between the MP2 ZPE corrected CCSD(T) BEs and electrostatic (ES, *blue circles* and polarization (PL, *red squares*) energy components for the clusters of Table 1

by Grabownski [48]. This point is better analyzed with the Bader's QTAIM [43] in the following section.

A final observation about this conformational M_2W_3 report: considering the valence bond model in its basic version [49], and taking into account only the PHB interactions, we may quickly notice that the number of possible M_2W_3 structures in the PES is very large; as the oxygen of the R-OH molecule has approximately a sp^3 hybrid character, each water molecule is able to form up to 4 directional tetrahedral HBs: two H acceptors and two H donors. Likewise, each methanol molecule can form up to 3 directional tetrahedral HBs: two H acceptors and one H donor. The possible combinations cause a large number of structures and, for a given structural motif, a large number of conformers. This increase even more if we observe that almost all this kind of clusters are dissymmetric, i.e., they do not have an improper rotation axis, therefore, they have optical isomers [50]. In this work, we have found 164 structures, but there are many others. Each run of the ASCEC program can find additional structures on this PES and, as the sampling is random, it improves as we increase the number of runs. However, even though each run of ASCEC program leaves out several structures, we have shown that (see Refs. [19, 21, 22, 28, 35, 36] among others), due to its selection criteria, our program is capable of finding the global minimum and several structures representing the major structural motifs, including some optical isomers.

3.2 Comparison with the W_5 clusters

Examining our M_2W_3 structures, we found that the hydrogen bond lengths in the case of PHBs are between 1.6 and 2.1 Å (a 0.5 Å range), while for SHBs, they are between 2.2 and 3.5 Å (a 1.3 Å range). That PHBs move in a narrow length range provide evidence that suggests that the PHBs are stronger and determine the structural cluster skeleton and that SHBs accommodate to the basic PHB structure, displaying with this a wider range of lengths. The

obvious evidence of this affirmation is the fact that for M_2W_3, the same basic structural motifs are found with respect to the case of W_5 [22], where there is no possibility of SHBs. The minor difference between our M_2W_3 results and our previous characterization of the W_5 PES is that for M_2W_3, we did not find the cage motif of the W_5 case, and we found for M_2W_3 PHB coiled chain-like structures not found in our W_5 study [22]. We constructed a M_2W_3 cage-like structure from the cage W_5 structure and optimized it. The resulting structure has a real lowest frequency and relative and binding MP2/6-311 ++G(d, p) energies of $\Delta E = 8.67$ kcal/mol and $BE = 24.93$ kcal/mol, respectively, i.e., it is situated between structures trimer + 1 + 1 cis and trimer + 1 + 1 trans (see Table 1), a relatively unstable structure (see Online resource for its Cartesian coordinates). This motif requires that 3 molecules are double PHB H donor.

For M_2W_3, we found five PHB coiled chain structures, two of which are mutual optical isomers. Those structures have SHBs (see the example in Fig. 1), which introduce some cycles in the structures, stabilizing the PHB chain-like configuration. For the W_n ($n = 5$–20) system, Parthasarathi et al. [51] have succeeded in getting linear chain-like dispositions, but they require to start from perfectly linear structures, which is improbable to reach in a stochastic methodology.

Another comparative observation is that we found for the M_2W_3 system the same five more stable motifs, within 3 kcal/mol, as for the W_5 case: puckered ring,envelope, tetramer/trimer, tricycle, and tetramer + 1. However, in the case of M_2W_3 systems, the BE are higher than in the case of W_5 clusters at the same level of theory. For example, at MP2/6-311 ++G(d, p) level, the W_5 BE are around 30.2, 29.1, 28.7, 27.7, and 26.6 kcal/mol for puckered ring, envelope, tetramer/trimer, tricycle, and tetramer + 1, respectively, against around 33.5, 32.5, 32.0, 31.5, and 31.0 kcal/mol of the M_2W_3 systems for the same respective structural motifs. This agrees with the electron donor effect of the methyl CH_3 group [23]. This group increases the electronic density over the oxygen atom enabling a better charge transfer toward the hydrogen atom of the other molecule with which it forms the HB, strengthening the intermolecular interaction.

It is known [48] that a greater HB electronic density means a greater covalent character of the interaction, which increases the bonding strength. This point can be better analyzed by Bader's QTAIM [43], which applied to HB closed shell interactions (those for which the Laplacian of the electronic density at the bonding critical points, $\nabla^2\rho_c$, is larger than zero) finds that this additional "covalent" factor strengths bonding, property that is expressed in some properties at the hydrogen bond critical points (HBCP), such as an increase in electron density, ρ_c, a shortening in the bond path lengths, BPLs, and an increase in the degree of covalency, indicated by lower values of total energy densities, H_c [48].

Table 2 shows comparative QTAIM data for selected pairs of PHB M_2W_3 and W_5 structures of four structural motifs. We included the electronic densities, ρ_c, potential energy densities, V_c, total energy densities, H_c, and ellipticities, ε, at the HBCP of each M_2W_3 and W_5 pair, which are related by the same PHB structural skeleton. We also included the respective bond path lengths, BPLs, and the binding energies, BE, at MP2/6-311 ++G(d, p) level for each structure. The labeling of the pairs of atoms between which there are HBCPs is detailed in Fig. 3, which corresponds to the topological molecular graphs of the selected W_5 and M_2W_3 pairs. Notice that in Fig. 3, we arranged each pair of structures in the same perspective to appreciate that they have the same PHB skeleton. Bond critical points, BCPs, ring critical points, RCPs, and cage critical points, CCPs, are indicated by green, red, and blue colors, respectively.

We can observe in Table 2 and Fig. 3 that the HBCPs of M_2W_3 structures, where the electronic density donor oxygens are assisted by the methyl groups (indicated as Hx–Oy–Met, where x and y are the numbers of the atoms in Fig. 3), have larger $\rho_c$values, smaller H_c, and shorter BPLs, with respect to the W_5 HBCPs, situated at the equivalent geometrical positions. For example, in the case of the puckered ring structure, $\rho_c = 0.0436$, $H_c = -0.0039$ and BPL = 3.26 for H6–O14–Met, and $\rho_c = 0.0434$, $H_c = -0.0038$ and BPL = 3.28 for H15–O20–Met, compared with $\rho_c = 0.0376$, $H_c = -0.0013$ and BPL = 3.36 for H4–O14, and $\rho_c = 0.0372$, $H_c = -0.0011$ and BPL = 3.36 for H15–O11 of the W_5 structure (all values in a.u.). As can be seen in Table 2 and in Fig. 3, the BEs of M_2W_3 systems are greater than the ones of W_5 at the same level of theory, as we indicated above. Those results, at least for the 4 examples showed, suggest that the inductive effect produced by the methyl groups reinforce the PHB bonding system by electronic density concentration at the BCPs, thus increasing the HBs degree of covalency. To be more precise, even though all the HBCPs found in this work fulfill the condition $\nabla^2\rho_c > 0$, i.e., they are closed shell interactions, some HBs have a degree of covalence when $H_c < 0$. ($|V_c| > G_c$, where G_c is the kinetic energy density at BCP) [48], i.e., they are able to reduce the energy of the system further by local charge concentration between the nuclei. In Table 2, we indicate this condition marking in bold the label of the atom pair involved. As we can see, for the structure series within each system, M_2W_3 and W_5, the general tendency is to increase the number of BCPs with covalent character as the BEs increase.

Table 2 QTAIM data of our pairs of the same M_2W_3 and W_5 PHBs selected structures shown in Fig. 3

Structure	$\rho_c \times 10^2$	$V_c \times 10^2$	$H_c \times 10^2$	$\varepsilon \times 10^2$	BPL
Puckered ring					
M2W3, BE = 33.6					
H6– O14–Met	4.36	−4.29	−0.39	3.90	3.26
H15–O20–Met	4.34	−4.27	−0.38	4.21	3.28
H3–O4	3.81	−3.61	−0.15	3.69	3.35
H9–O1	3.76	−3.52	−0.13	4.31	3.36
H21–O7	3.64	−3.39	−0.08	8.07	3.39
W5, BE = 30.2					
H4–O14	3.76	–3.53	−0.13	3.67	3.36
H1–O5	3.73	−3.51	−0.12	3.81	3.36
H7–O2	3.73	−3.49	−0.12	4.19	3.36
H15–O11	3.72	−3.49	−0.11	3.97	3.36
H12–O8	3.50	−3.22	−0.03	8.74	3.40
Envelope					
M2W3, BE = 32.5					
H2–O20-Met	4.24	−4.16	−0.33	4.49	3.28
H21–O14-Met	4.24	−4.09	−0.35	6.09	3.30
H9–O1	3.82	−3.58	−0.16	5.62	3.35
H15–O4	3.40	−3.10	−0.02	3.45	3.45
H6–O7	3.34	−3.03	0.04	9.84	3.44
C–H12–O7	0.44	−0.27	0.05	11.42	5.46
W5, BE = 29.1					
H6–O14	3.69	−3.41	−0.11	6.05	3.38
H13–O11	3.61	−3.38	−0.06	4.88	3.38
H12–O2	3.56	−3.25	−0.07	7.44	3.40
H3–O8	3.42	−3.13	−0.01	4.63	3.42
H7–O5	3.37	−3.09	0.04	10.13	3.42
Tricycle					
M2W3, BE = 31.7					
H21–O14–Met	4.83	−4.85	−0.64	4.79	3.21
H15–O7	3.93	−3.62	−0.26	5.63	3.39
H3– O20–Met	2.94	−2.51	0.10	5.77	3.57
H5–O20–Met	2.68	−2.20	0.14	7.08	3.65
H8–O4	2.36	−1.88	0.15	1.99	3.78
H9–O1	2.32	−1.86	0.16	6.71	3.79
C–H12–O4	0.27	−0.17	0.05	16.77	5.86
W5, BE = 27.7					
H3–O14	4.00	−3.73	−0.27	4.62	3.35
O2–H9	3.91	−3.71	−0.19	6.17	3.33
H4–O8	2.47	−1.99	0.20	5.05	3.69
O11–H13	2.43	−1.95	0.14	2.08	3.76
O8–H10	2.34	−1.85	0.20	7.60	3.74
O5–H15	2.26	−1.80	0.17	6.60	3.81
Tetramer + 1					
M2W3, BE = 29.8					
H2–O4	4.18	−3.98	−0.32	2.27	3.31
H8–O14-Met	3.82	−3.57	−0.16	4.29	3.37
H15–O1	3.68	−3.43	−0.10	3.60	3.39
H5–O7	2.76	−2.32	0.13	2.72	3.62
H6–O20–Met	2.75	−2.31	0.10	2.73	3.66
C–H18–O7	0.46	−0.29	0.06	9.69	5.35
C–H17–O1	0.29	−0.17	0.05	26.98	5.74
C–H12–H17–C	0.24	−0.13	0.05	174.43	6.02
W5, BE = 26.6					
H4–O14	3.96	−3.77	−0.22	3.49	3.33
H10–O5	3.60	−3.31	−0.08	3.24	3.40
H1–O11	3.36	−3.01	0.01	3.33	3.45
H13–O2	2.94	−2.51	0.11	3.17	3.56
H15–O8	2.40	−1.93	0.22	4.56	3.70

All data in a.u. BEs at MP2/6-311 ++G(d, p) level in kcal/mol

Although the degree of covalency is higher (H_c more negative) for methyl-assisted HBs, it is interesting to note that where a double H acceptor is involved (double electron density donor), this effect is attenuated. For example, compare in Table 2, the ρ_c and H_c values of the double H acceptor oxygen O20 in the tricycle M_2W_3 structure with its equivalent double H acceptor oxygen O8 in the tricycle W_5 structure. Notice also that the HBCP involved has no degree of covalency ($H_c > 0$).

Additionally, the tetramer + 1 case constitutes evidence of covalency loss when there are double H donor water molecules: notice in Fig. 3 and in Table 2 that in the M_2W_3 structure, the water molecule H5–O4–H6 is double H donor and also H acceptor. This produces a loss of the degree of covalency at the HBCPs where this molecule is H donor (H6–O20–Met = +0.001 a.u. and H5–O7 = +0.0013 a.u.). The same applies in the case W_5 (see the H13–O14–H15 water molecule). Those facts favor the statement made in the previous section on the weakening of the hydrogen bonding when there are double H acceptors or double H donors.

Another related observation is that the V_c values of the M_2W_3 structures are, in general, lower (more negative) than the W_5 ones at the equivalent geometrical positions, especially in the HBCP assisted by the methyl groups. The total sum of V_c values for each M_2W_3 structure are −0.190, −10182, −0.171, and −0.162 for puckered ring, envelope, tricycle, and tetramer + 1, respectively, which are lower than the W_5 sums for the same PHBs motifs: −0.184, −0.163, −0.150, and −0.145. Note also that within each system, M_2W_3 and W_5, these sums are more negative as the structure has higher BE. Espinosa et al. [52] have proposed a proportionality between the hydrogen bond energy at the BCP, B_c, and the potential energy density at BCP: $B_c = -\frac{1}{2}V_c$. This relationship has been successfully applied, for example, in ice phases HB systems [53]. On

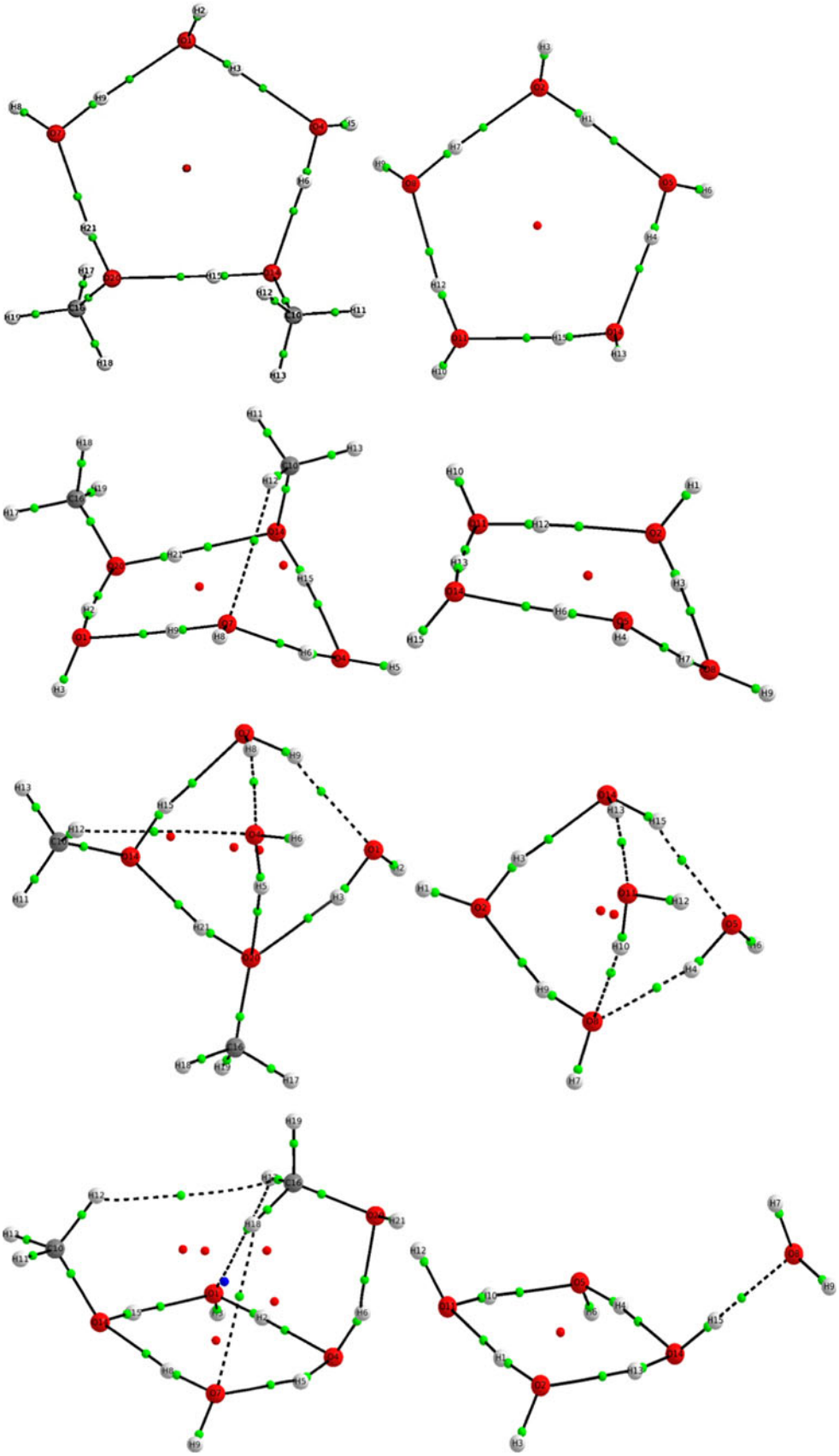

Fig. 3 Topological molecular graphs of four selected W_5 and M_2W_3 structural motifs pairs. Bond critical points, ring critical points, and cage critical points are indicated by *green*, *red,* and *blue colors*, respectively. BPLs are indicated as *solids* or as *dotted lines*

this basis, we can think that there must be some degree of proportionality between local binding energy sums, $\sum B_c = -\frac{1}{2}\sum V_c$, and the net BEs. Figure 4 suggests this relationship for the structures of Table 1, using the BEs at the CCSD(T)/6-311 ++G(d, p) level (and the quantity $2\sum B_c = -\sum V_c$). We have also plotted in the same figure $\sum \rho_c$ versus BEs. Even though $\sum \rho_c$ is not exactly a measure of the covalency degree, it should be proportional to the covalency; therefore, the correlation showed in Fig. 4 indicates, approximately, that as the total bonding covalency degree increases, the structures are more stable. The fluctuations showing in the $\sum \rho_c$ versus BE behavior tell us that there are additional stability and instability factors, such as the other energy components: polarization, delocalization, correlation, exchange, repulsion, and structural stress.

The least stable structure found is the tetramer + 1 shown in Fig. 5a. This structure also exhibits the smallest

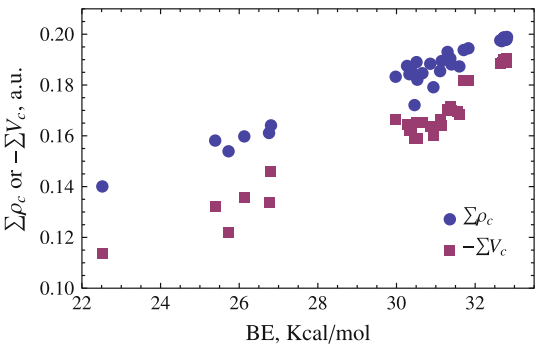

Fig. 4 Correlation between the MP2 ZPE corrected CCSD(T) BEs and $-\sum V_c$ (*red squares*), and $\sum \rho_c$ (*blue circles*) at HBCPs for the structures of Table 1

values for $-\sum V_c$ and $\sum \rho_c$. Notice that this structure has three important factors of instability: it has a small ring (cyclic tetramer, a stressed structure compared to the cyclic pentamer), it has bond pairs of opposing dipoles (electrostatically disfavored), and it has two double H donors and two double electron pair donors, which reduce the electron density concentration of the tetramer H bonds (covalently disfavored).

By observing in Table 2, the QTAIM quantities of the secondary interactions (SHB) indicated as C–Hx–Oy (x, y, number labels) in M_2W_3 envelope, tricycle, and tetramer + 1 structures, we can see that they are very weak closed shell interactions: they show very small ρ_c and $|V_c|$ values, positive H_c values, high values for ε and BPLs. Elevated values of ε indicate instability of the HBCPs. In the case of the BPLs, if we make a rough estimation, we can observe that none of them is smaller than the sum of the van der Waals radii, which is about 5.0 a.u. [54, 55]; therefore, according to the mutual penetration criteria (H and O) of hydrogen bonding [43, 56], those SHB interactions are not true HBs. This weakness in SHBs suggests that the PHB interactions are pivotal in determining the basic structure, mainly by directional electrostatic interactions over SHBs (the covalence and the other attractive interactions would help to stabilize the structures even more). The SHBs interactions approximately fit the structural conditions imposed by the PHB system and, in most cases, would contribute only marginally to the structural geometry and its stability. However, there could be cases among the more unstable clusters, where the SHB interactions are crucial, as we found for the nonlinear (coiled) PHB chain-like motifs. Notice that we can build a nonlinear PHB chain-like structure by replacing a PHB in a

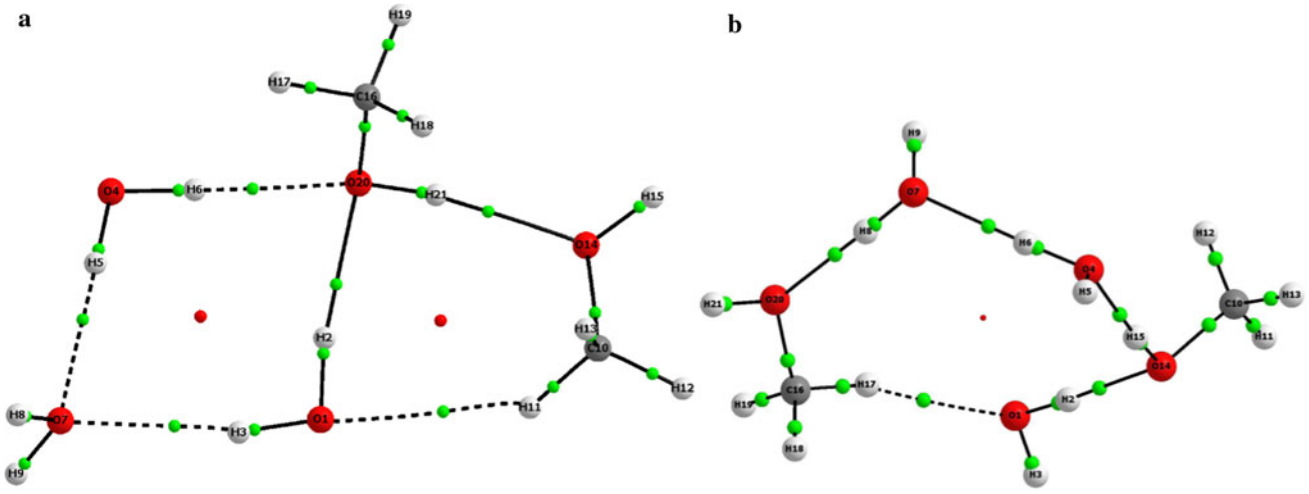

Fig. 5 Topological molecular graphs of (**a**) the least stable structure found, and (**b**) a nonlinear PHB chain-like structure. Bond critical points, ring critical points, and cage critical points are indicated by *green*, *red,* and *blue colors*, respectively. BPLs are indicated as *solids* or as *dotted lines*

puckered ring structure by a SHB. For example, in the puckered structure, 4 of Fig. 1, if we replace a PHB between the hydrogen of the OH group of a methanol molecule and an oxygen atom of a water molecule by an hydrogen of the -CH_3 group of the same methanol molecule and the oxygen atom of the same water molecule, we obtain the structure whose topological molecular graph and QTAIM data are shown in Fig. 5b and Table 3, respectively. We observe in Table 3 that the H_c values are an order of magnitude larger (less negative) than for the puckered ring structure shown in Table 2. This means a substantial loss of covalency degree and, as seen in the BE value, a loss in stability. Other HBCP QTAIM features indicate the same: larger V_c, BPL, and ε values and lower ρ_c values. Notice also that for the SHB case (C–H17–O1) in Table 3, the H_c positive value is larger than the H_c values of the C–Hx–Oy interactions of the structures of Table 2. However, its ρ_c value is larger and BPL, V_c, and ε are smaller with respect to the values in Table 2. This indicates that even though this SHB of this chain-like structure has no degree of covalency, it is stronger than the SHBs of the other structures showed. In fact, the BPL found is smaller than the van der Waals approximated radius (5.0 a.u.), which classified this interaction as a true HB [43, 54, 55]. This case shows that we cannot dismiss the role of the SHB interactions, which although weaker than PHB interactions, could have the ability to entrap structures in alternative local minima. This can be very important in biological systems, where some biochemical subtleties cause large biological effects.

4 Conclusions

1. The determining factor of the structure, stability and bonding in the $(Methanol)_2(Water)_3$ system is mainly the distribution of the O–H···O PHBs. The C–H···O SHBs play a secondary role and preferably "accommodate" to the dominating PHB structures.
2. As was evidenced by the energy decomposition and by the QTAIM analysis in relation to the BEs values, the stability of the found clusters is strongly correlated with the electrostatic binding component and with the degree of covalency.
3. Related to the above points, we can say that within those PHBs systems, the geometrical motifs variety, nature, and stabilities depend mainly on 2 factors: (a) the sequence and spatial configuration of interacting dipoles $[(\delta^-)O–H(\delta^+)\cdots\ (\delta^-)O–H(\delta^+)]$, and (b) the overlapping between the appropriate electronic densities to give the binding local densities. Consecutive quasi-planar and closed sequence of dipoles, in which each molecule is H acceptor and H donor only once, gives the more energetically favorable motifs.
4. The main instability factors in the M_2W_3 clusters are (a) planarity loss, (b) the decrease in the rings size (5 → 4, 3), (c) presence of double H donor or double H acceptor molecules, and (d) absence of rings. Those factors affect a better aligning of dipoles, affect the cooperative effects achieved in cyclic system of dipoles, affect the degree of overlap between the electron pair and electron densities associated with the hydrogen terminal of the H–O bond, and the local electron densities between the atoms linked by HBs.
5. The methyl groups increase the structural isomerism possibilities in the M_2W_3 pentamers. They are also important in their stability: They induce an increased electron density between the atoms linked by HB (conclusion also reached by Subramanian et al. [23]), thereby increasing the covalent component and electrostatic favorable redistribution to the overall stability.
6. The methyl groups practically do not influence the more stable structures, which result in the same geometrical motifs as the W_5 case. However, they can play a fundamental role in the less stable structures. One example is the case of the PHB coiled chain-like motif, which is totally unstable in the methyl absent pure water pentamers, but it is possible by the SHBs in the water–methanol studied clusters, where the SHBs show a true hydrogen bond stabilizing character. Therefore, the SHBs could become an important structural factor in some cases. This fact should be taken into account, especially in biochemical systems.

Table 3 QTAIM data for the coiled chain-like M2W3 structure shown in Fig. 5b

Structure	$\rho_c \times 10^2$	$V_c \times 10^2$	$H_c \times 10^2$	$\varepsilon \times 10^2$	BPL
M2W3, BE = 26.4					
H6–O7	3.61	−3.35	−0.06	4.89	3.38
H15–O4	3.54	−3.28	−0.04	4.41	3.41
H2–O14	3.51	−3.17	−0.04	4.75	3.43
H8–O20	3.46	−3.18	−0.01	5.81	3.41
C–H17–O1	1.24	−0.79	0.12	8.98	4.42

All data in a.u. BE at MP2/6-311 ++G(d,p) level in kcal/mol

Acknowledgments C.Z.H. and A. R. are grateful to Universidad de Antioquia for partial financial support through Estrategia de Sostenibilidad 2013-2014 project, and C.Z.H. thanks Proyecto CIEN-CODI IN10184CE. S.J gratefully acknowledges the support of the One Hundred Talents of Hunan program for support and the aid program for Science and Technology Innovative Research Team in Higher Educational Institutions of Hunan Province. The National Natural Science Foundation of China is also gratefully acknowledged, project approval number: 21273069.

References

1. Xantheas SS (2010) Recent theoretical and experimental advances in hydrogen bonded clusters. Nato Science Series: C Mathematical and Physical Sciences, Volume 561 Kluwer Academic Publishers, Dordrecht, The Netherlands
2. Schuster P, Wolschann P (1999) In: Schuster P, Wolschann P (eds) Hydrogen bonding: from small clusters to biopolymers. Springer, Wien
3. Guo JH, Luo Y, Augustsson A, Kashtanov S, Rubensson JE, Shuh DK, Agren H, Nordgren J (2003) Phys Rev Lett 91:157401–157402
4. Ruckenstein E, Shulgin IL, Tilson L (2005) J Phys Chem A 109:807
5. Teschke O, de Souza EF (2005) Chem Phys Lett 403:95
6. Teschke O, de Souza EF (2005) Phys Chem Chem Phys 7:3856
7. Perera A, Mazighi R, Kežíc BJ (2012) Chem Phys 136:174516
8. Bagchi B (2012) Chem Phys Lett 9:1
9. Dougherty RC, Howard LN (1998) J Chem Phys 109:7379
10. Lin K, Zhou X, Luo Y, Liu S (2010) J Phys Chem B 114:3567
11. Tamenori Y, Okada K, Takahashi O, Arakawa S, Tabayashi K, Hiraya A, Gejo T, Honma K (2008) J Chem Phys 128:124321
12. Kumagai T (2012) Visualization of hydrogen-bond dynamics: water-based model systems on a Cu(110) surface. Springer, Japan
13. Marechal Y (2007) The hydrogen bond and the water molecule: the physics and chemistry of water. Aqueous and Bio-Media, Elsevier
14. Eisenberg D, Kauzmann W (2005) The structure and properties of water. Oxford University Press, Oxford
15. Xantheas SS (2000) Chem Phys 258:225
16. Goldman N, Fellers RS, Brown MG, Braly LB, Keoshian CJ, Leforestier C, Saykally RJ (2002) J Chem Phys 116:10148
17. Nielsen IMB, Seidl ET, Janssen CL (1999) J Chem Phys 110:9435
18. Ren P, Ponder JW (2005) J Phys Chem B 107:5933
19. Hincapié G, Acelas N, Castaño M, David J, Restrepo A (2010) J Phys Chem A 114:7809
20. Han G, Ding Y, Qian P, Zhang C, Song W (2012) Int J Quantum Chem. doi:10.1002/qua.24352
21. Pérez J, Hadad C, Restrepo A (2008) Int J Quantum Chem 108:1653
22. Ramirez F, Hadad CZ, Guerra D, David J, Restrepo A (2011) Chem Phys Lett 507:229
23. Mandal A, Prakash M, Kumar RM, Parthasarathi R, Subramanian V (2010) J Phys Chem A 114:2250
24. Stockman PA, Blake GA, Lovas FJ, Suenram RD (1997) J Chem Phys 107:3782
25. Iosue JL, Benoit DM, Clary DC (1999) Chem Phys Lett 301:272
26. Jursic BS (1999) J Mol Struct Theochem 466:203
27. Gonzáles L, Mó O, Yáñez M (1998) J Chem Phys 109:139
28. Mejía SM, Espinal JF, Restrepo A, Mondragón F (2007) J Phys Chem A 111:8250
29. Mejía SM, Espinal JF, Mondragón F (2009) J Mol Struct Theochem 901:186
30. Mejía SM, Flórez E, Mondragón F (2012) J Chem Phys 136:144306
31. Raina G, Kulkarni GU (2001) Chem Phys Lett 337:269
32. Tsuneishi S (2011) Import Tuner magazine, January
33. Snyder LR, Kirkland JJ, Dolan JW (2009) Introduction to modern liquid chromatography. Wiley, New York
34. Pérez J, Restrepo A (2008) ASCEC V-02: Annealing Simulado con Energía Cuántica. Property, Development and Implementation: Grupo de Química–Física Teórica, Instituto de Química, Universidad de Antioquia: Medellín, Colombia
35. David J, Guerra D, Restrepo A (2009) J Phys Chem A 113:10167
36. Murillo J, David J, Restrepo A (2010) Phys Chem Chem Phys 12:10963
37. Liedl K, Sekušak S, Mayer E (1997) J Am Chem Soc 119:3782
38. Peterson K, Dunning P (1995) J Chem Phys 102:2032
39. Xantheas S (1996) J Chem Phys 104:8821
40. Feyereisen M, Dixon D (1996) J Phys Chem 100:2993
41. Frisch MJ et al (2004) GAUSSIAN 03, Revision E.01, Gaussian, Inc., Wallingford CT
42. AIMAll (Version 10.09.12), T A Keith (2010) (aim.tkgristmill.com)
43. Bader R (1994) Atoms in molecules: a quantum theory. Oxford University Press, USA
44. Gillespie RJ, Hargittai I (2012) (1996) The VSEPR model of molecular geometry. Dover Books on Chemistry, United States
45. Hoffmann R, von Ragué Schleyer P, Schaefer HF (2008) Angew Chem Int Edit 47:7164
46. Su P, Li H (2009) J Chem Phys 131:014102
47. Kitaura K, Morokuma K (1976) Int J Quantum Chem 10:325
48. Grabowski S (2011) J Chem Rev 111:2597
49. Shaik SS, Hiberty PC (2008) A chemist's guide to valence bond theory. Wiley-Interscience, New Jersey
50. Cotton FA (1990) Chemical applications of group theory. John Wiley & Sons, New York
51. Parthasarathi R, Elango M, Subramanian V, Sathyamurthy N (2009) J Phys Chem A 113:3744
52. Espinosa E, Molis E, Lecomte C (1998) Chem Phys Lett 285:170
53. Jenkins S, Morrison I (2000) Chem Phys Lett 317:97
54. Oliveira BG, Vasconcellos MLAA (2006) J Mol Struct Theochem 774:83
55. Bondi A (1964) J Phys Chem 68:441
56. Koch U, Popelier PLA (1995) J Phys Chem 99:9747